geoconvention
Calgary • Canada • May 7-11 2018

Seismic Hazard and Cellular Automaton

Edouard Kravchinsky[1], Mirko van der Baan[1], and Javad Kazemian
1: Dept. of Physics, CCIS, University of Alberta, T6G 2E1, Canada

Summary

This presentation focuses on investigating the effects of inhomogeneities and varied structures on earthquake sequences. We find that increasing the percentage of inhomogeneities modifies both the overall shape and slope of the frequency-magnitude relation. Different heterogeneous shapes and structures can either suppress or strengthen these changes. Furthermore, we develop an analytical predictive model which we compare to our simulated results. We notice deviations between our predictions and simulated results suggesting a more complicated relation between earthquake sequences and spatial arrangement of inhomogeneities.

Introduction

The topic of industrial activity possibly inducing earthquakes remains an active research subject. The cellular automaton (CA) model is simple, yet capable of producing complex patterns also observed in earthquakes (Bak et al., 1988; Olami et al., 1992). The CA model remains a powerful method for studying earthquake dynamics such as magnitude and scaling, clustering, spatial heterogeneities, foreshocks and aftershocks and so forth (Castellaro and Mulargia, 2001; Georgoudas et al., 2007; Dominguez et al., 2013; Kazemian et al., 2015).

Numerically studying earthquakes with CA models stems from Burridge and Knopoff (1967) and their laboratory experiments of earthquake sequences. In order to further study the effect of friction Burridge and Knopoff implemented a numerical model derived from the equations of motion along with a friction law. Later, Rundle and Brown (1991) presented a 2-D version of the numerical model. The model is constructed from interconnected homogeneous masses and springs, see Figure 1. Overtop the model is a rigid loader plate that acts as a constant sliding rate to each mass via a rigid coupling spring. From the model, a pattern of stick-slip friction or cohesion-decohesion of the coupled blocks was observed as sites failed by sliding. These slipping occurrences would create chain reactions across the lattice. We investigate how inhomogeneities and varied structures influence seismic patterns.

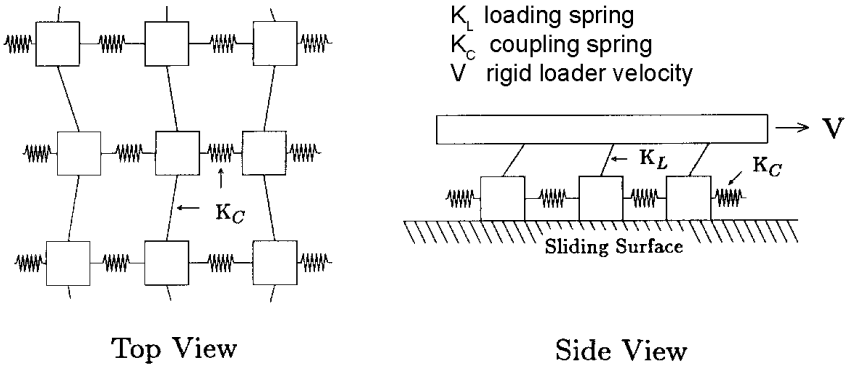

Figure 1: The 2-D spring-block model with homogeneous masses and springs.
Left: The masses are represented as white blocks interconnected by identical spring constants K_C.
Right: A rigid loader plate V applies a constant sliding rate to each mass via a rigid loading spring K_L.
Modified schematic diagram of the 2-D Burridge-Knopoff spring-block model Rundle and Brown (1991).

Theory and Method

The 2-D cellular automaton is composed of L by L hexagonal cells. Each lattice cell is assigned a residual stress threshold (σ_R) and a failure threshold (σ_F). We impose quenched randomness on the residual stress where $\sigma_R \pm \eta$ such that random variations exist from one cell to another. At initialization, an internal stress σ_i is randomly assigned to each cell such that $\sigma_R < \sigma_i < \sigma_F$. The effects of inhomogeneities are incorporated through asperities that have an increased failure threshold σ_F compared to the normal cells.

The entire lattice is searched for a cell closest to failure or having the least stress difference of $min(\sigma_F - \sigma_i)$. This minimum stress difference is added to each cell of the lattice also known as a plate update time step (t_{pu}). Consequently, the cell closest to failure breaks and releases its total stress of $\sigma_F - \sigma_R$. A fraction of the stress, given by $(1-\alpha)[\sigma_F - \sigma_R]$, is equally redistributed among surrounding cells within a radius of R cells. Therefore, α is the dissipation parameter that lies in-between $0 < \alpha \leq 1$. The $\alpha[\sigma_F - \sigma_R]$ fraction of the released stress is permanently lost. Subsequently, a surrounding cell may fail if it gains enough stress such that $\sigma_i \geq \sigma_F$. If so, the process of total stress redistributing and dissipation for the newly failed cell is repeated. Once all cell failures have occurred, in other words $\sigma_i < \sigma_F$ for all cells, the plate update time step is increased by $t_{pu} = t_{pu} + 1$. The size of each event (s) is the total cumulative number of cell failures for a given plate update time step; this is how we simulate our time series of total cumulative cell failures per plate update.

In seismology, the Gutenberg-Richter (GR) relation between earthquake magnitude and frequency can be re-expressed as a power law proportional to the seismic moment M_0 given as

$$N_{M_0} \sim N_T {M_0}^{-2/3b}, \text{ where } N_T = 10^a, \qquad (1)$$

and N_{M_0} is the total number of events with a moment greater or equal to M_0, and N_T is the total seismicity of the region (Serino et al., 2011). The constant a is a measure of the regional level of seismicity, whereas the constant b is largely determined by the underlining stress regime (Pacheco et al., 1992; Frohlich and Davis, 1993). The universal scaling relation of Equation 1 has been observed and studied in various models, including the Burridge-Knopoff slider block model and the CA implementations (Burridge and Knopoff, 1967; Rundle and Brown, 1991; Olami et al., 1992). These CA models with long-range stress transfer exhibit clustering scaling that can be described by the Fisher droplet model distribution as

$$n_s = n_0 \exp(\Delta h \cdot s) / s^{\tau}, \qquad (2)$$

where n_s is the non-cumulative count of failed cells with size s (Fisher, 1967; Klein et al., 2000). As such, n_0 is a measure of the seismicity, whereas Δh is the distance from the spinodal, and $\tau = 3/2$ for systems with long-range stress transfer (Klein et al., 2000; Klein et al., 2007). Therefore, constants n_0 and Δh of Equation 2 are analogues to constants N_T and b of Equation 1.

Serino et al. (2011) determined a dependence of n_0 and Δh on q, where in their model q was a fraction of sites acting as stress sinks. Similarly, we have fit n_s using weighted non-linear least-squares fit for n_0 and Δh to Equation 2. We have found that Δh can be approximated by

$$\Delta h \approx \alpha^{5/2} \qquad (3)$$

for a wide range of α values. Furthermore, the total number of failures, n_{tot}, over an area containing L^2 cells is given as

$$n_{tot} = \Delta\sigma L^2 / [(\sigma_F - \sigma_R)\alpha], \qquad (4)$$

where $\Delta\sigma$ is the stress added, α the dissipation parameter with σ_F and σ_R being the failure and residual stress thresholds, respectively. As Equation 2 is a non-cumulative distribution only a fraction of the total number of failures, $n_{s=1}/n_{tot}$, are events of size $s = 1$. Fitting data suggests that the number of events of size $s = 1$ can be approximated as

$$n_{s=1} \approx [0.9807\alpha^{1.744} + 0.01308] \cdot n_{tot}, \qquad (5)$$

where α is the dissipation parameter and n_{tot} is the total number of failures of Equation 4. We can solve for n_0 by substitution $n_{s=1}$ (Equation 5) into the Fisher droplet model (Equation 2) for $s = 1$. Thereafter, we find that

$$n_0 \approx [\Delta\sigma L^2(0.9807\alpha^{1.744} + 0.01308)]/[\alpha(\sigma_F - \sigma_R)\exp(-\alpha^{5/2})]. \qquad (6)$$

Finally, substitution of Equations 3 & 6 into Equation 2 gives us

$$n_s \approx [\Delta\sigma L^2 \exp(\alpha^{5/2}(1-s))(0.9807\alpha^{1.744} + 0.01308)]/[\alpha(\sigma_F - \sigma_R)s^{3/2}], \qquad (7)$$

which is an approximate predicted distribution of the number of events, n_s, of size s as a function of known model parameters $\Delta\sigma$, L, α, σ_F, and σ_R. This allows us to compare the predicted model to our simulated results. To predict effects of inhomogeneities we utilize Equation 7 by considering the inhomogeneous models as a sum of two parts; one area part with normal cells, and another part with asperity cells. Therefore, the predicted distribution is the sum of two independent parts.

Examples

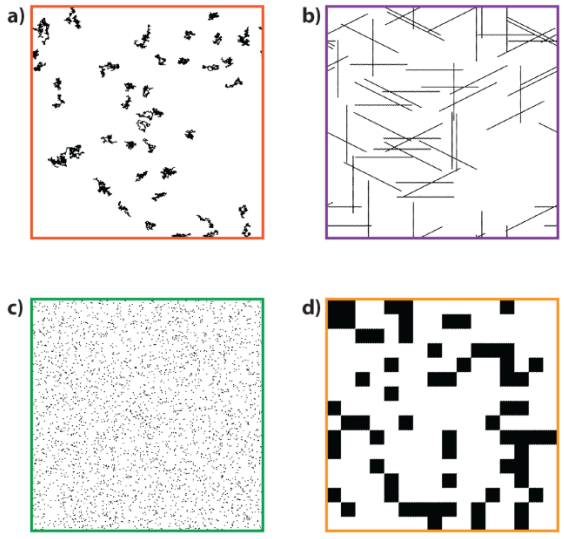

Figure 2: Various inhomogeneous structure models with normal cells ($\sigma_F = 1.0$) in white and asperities ($\sigma_F = 11.0$) in black. Models shown have asperity percentages ranging from a) - c) 5% and d) 25%. Structures include a) random walk, b) linear fractures, c) uniformly distributed asperities of block width 1, and d) uniformly distributed asperities of block width 16. The total lattice size is *256* by *256* elements.

The shape of inhomogeneous structures can greatly influence the statistics of the model. Therefore, we varied the spatial distribution of asperities within the lattice system. All model parameters, such as $R = 16$, $\alpha = 0.05$, $\Delta\sigma$, L, σ_F, and σ_R were kept identical between all models. Four of the cases vary in structural shapes with three models having 5% percent of asperities (frac, lin frac, rnd B_1) and one model containing 25% of asperities (rnd B_{16}), see Figure 2. Structures include random walk (frac), linear fractures (lin frac), blocks of width 1 (B_1), and blocks of width 16 (B_{16}). A benchmark model containing 0% asperities is included in the results. The frequency-magnitude plot for the five cases is shown in Figure 3 with the prediction for the no asperity model (no asp) and the inhomogeneous model with blocks of width 16 (B_{16}) plotted as solid and dashed black curves, respectively. The predicted curve for the inhomogeneous models of frac, lin frac, and rnd B_1 is plotted as a dotted black curve as they all contain 5% inhomogeneities. Generally, as the percentages of heterogeneities increase we

observe a slight decrease in small to medium sized events (s<10^3), but an increase in the range of larger size events (s>10^3), see Figures 3. Although model B_{16} contains 25% asperities the larger blocks better suppress the production of small sized events when compared to both the frac and lin frac models. The rnd B_1 model is dissimilar to all other results in many regards. For the rnd B_1 model we observe a significant reduction in medium size events (10^2<s<10^3) with an increased maximum magnitude range. In Figure 3, the predicted distributions are plotted as solid black for the no asp model, dotted for the 5% asperity models and dashed for the 25% asperity model. It becomes apparent that predicting the frequency-magnitude distributions for the heterogeneous systems is not as simple as assuming a combination of two simpler distributions. Particularly, we showed an example of how various spatial distributions of asperities can greatly impact seismic hazard and maximum expected magnitudes. These results further support the idea that the underlining physics originate from the interactions between the normal and asperity cells rather than a combination of two independent systems.

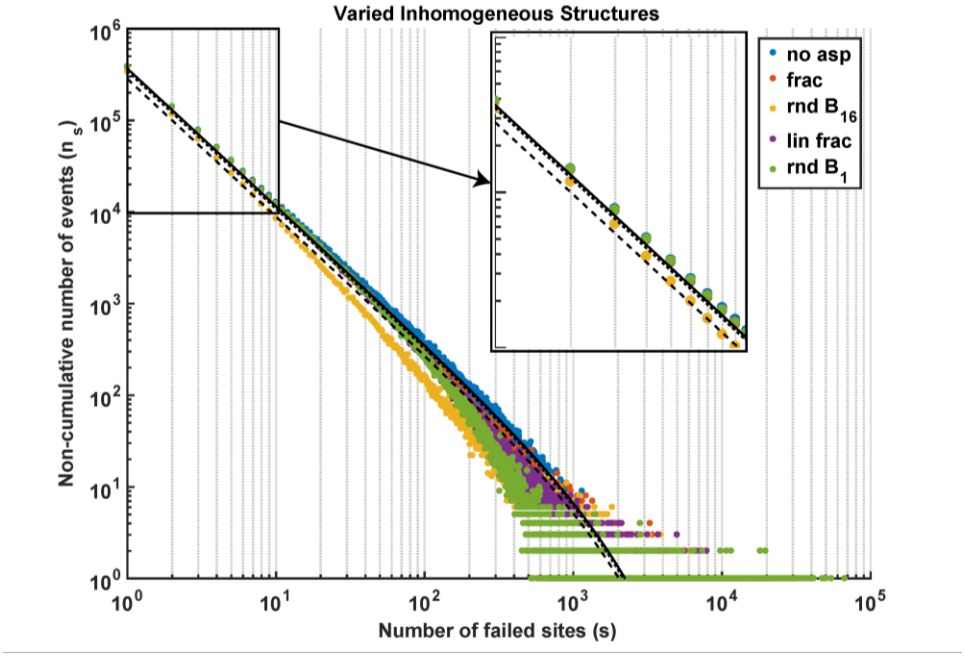

Figure 3: Non-cumulative frequency-magnitude distribution for models with no inhomogeneities (blue), and models with inhomogeneous structures including fractures (orange), blocks of width 16 (yellow), linear fractures (purple), and blocks of width 1 (green). The predicted frequency-magnitude distributions are plotted as solid, dotted and dashed black curves. The solid black curve is the no asp model with the dotted black curve slightly below belonging to the the frac, lin frac and rnd B_1 model. The dashed black curve is the rnd B_{16} predicted model. Actual model structures are shown in Figure 2.

Conclusions

The role of asperities is complicated, but in general these inhomogeneities add rigidity to the system. Overall, we observe a decreased occurrence of smaller sized events with an increased or extended range in the occurrence of largest sized events. We also determined that the extent of these changes is strongly influenced by the underlining heterogeneous structures. Furthermore, the addition of asperities can introduce spatiotemporal clustering that greatly contribute to increasing the range and expected maximum magnitudes. The precise role of structures is still under investigation, but the asperities size and shape appear to contribute greatly to changes in seismicity. Lastly, any future predictive models must try to capture the interaction that occurs between normal cells and inhomogeneities.

Acknowledgements

The authors would like to thank the sponsors of the Microseismic Industry Consortium for financial support.

References

Bak, P., Tang, C., & Wiesenfeld, K. (1988). Self-organized criticality. *Physical review A*, 38(1), 364.

Burridge, R., & Knopoff, L. (1967). Model and theoretical seismicity. *Bulletin of the Seismological Society of America*, 57(3), 341-371.

Castellaro, S., & Mulargia, F. (2001). A simple but effective cellular automaton for earthquakes. *Geophysical Journal International*, 144(3), 609-624.

Dominguez, R., Tiampo, K., Serino, C. A., & Klein, W. (2013). Scaling of earthquake models with inhomogeneous stress dissipation. *Physical Review E*, 87(2), 022809.

Fisher, M. E. (1967). The theory of equilibrium critical phenomena. *Reports on Progress in Physics*, 30(2), 615.

Frohlich, C., & Davis, S. D. (1993). Teleseismic *b* values; Or, much ado about 1.0. *Journal of Geophysical Research: Solid Earth*, 98(B1), 631-644.

Georgoudas, I. G., Sirakoulis, G. C., & Andreadis, I. (2007). Modelling earthquake activity features using cellular automata. *Mathematical and Computer Modelling*, 46(1), 124-137.

Kazemian, J., Tiampo, K. F., Klein, W., & Dominguez, R. (2015). Foreshock and Aftershocks in Simple Earthquake Models. *Physical Review Letters*, 114(8), 088501.

Klein et al., (2000), in Geocomplexity and the Physics of Earthquakes, edited by J. B. Rundle et al. *American Geophysical Union*.

Klein, W., Gould, H., Gulbahce, N., Rundle, J. B., & Tiampo, K. (2007). Structure of fluctuations near mean-field critical points and spinodals and its implication for physical processes. *Physical Review E*, 75(3), 031114.

Olami, Z., Feder, H. J. S., & Christensen, K. (1992). Self-organized criticality in a continuous, nonconservative cellular automaton modeling earthquakes. *Physical Review Letters*, 68(8), 1244.

Pacheco, J. F., Scholz, C. H., & Sykes, L. R. (1992). Changes in frequency–size relationship from small to large earthquakes. *Nature*, 355(6355), 71-73.

Rundle, J. B., & Brown, S. R. (1991). Origin of Rate Dependence in Frictional Sliding. *Journal of Statistical Physics*, 65(1), 403-412.

Serino, C. A., Tiampo, K. F., & Klein, W. (2011). New Approach to Gutenberg-Richter Scaling. *Physical Review Letters*, 106(10), 108501.